Journal of Molecular Structure 1251 (2022) 132033

Contents lists available at ScienceDirect

Journal of Molecular Structure

journal homepage: www.elsevier.com/locate/molstr

Synthesis and structure of azelastine-*N*-oxides

Benjamin Brandes[a], Jan H. Halz[b], Kurt Merzweiler[b], Hans-Peter Deigner[c], René Csuk[a,*]

[a] Martin-Luther-University Halle-Wittenberg, Organic Chemistry, Kurt-Mothes-Str. 2, Halle (Saale) D-06120, Germany
[b] Martin–Luther-University Halle-Wittenberg, Inorganic Chemistry, Kurt-Mothes-Str. 2, Halle (Saale) D-06120, Germany
[c] Furtwangen University, Institute of Precision Medicine, Medical and Life Sciences Faculty, Jakob-Kienzle-Straße 17, Villingen-Schwenningen D-78054, Germany

ARTICLE INFO

Article history:
Received 13 October 2021
Revised 3 November 2021
Accepted 18 November 2021
Available online 29 November 2021

Keywords:
Azelastine
N-oxides
Structure

ABSTRACT

Azelastine is among the most frequently used drugs; however, knowledge and solid data about its metabolites are scarcely found in literature. Thus, microsomal oxidation of azelastine is thought to produce the corresponding *N*-oxides, However, until now these products had never been produced in significant amounts. By oxidation of azelastine with H_2O_2, these *N*-oxides were now prepared in racemic form for the first time and were fully characterized. Their structure was additionally confirmed by a single crystal X-ray analysis. Both *N*-oxides were found to be non-cytotoxic in SRB assays.

1. Introduction

Azelastine [1,2], along with cetirizine and loratadine (Fig. 1), is one of the most frequently used drugs for the therapy of allergic rhinitis. In 2017, there were more than one million prescriptions in the USA, and in 2019 alone, US. sales amounted to US $18 million [3]. However, this second-generation antihistamine ("nonsedating") came also recently into the focus of scientific and public interest for another reason: azelastine is currently being tested in a clinical trial series to demonstrate its anti-viral efficacy in COVID-19 positive patients [4–12].

In former times, *N*-oxides were often regarded as side products derived from parent drugs generated by hepatic metabolism. Nowadays, they are conceived as nitric oxide mimics or bioisosteres of the carbonyl group; they may act as hypoxic-selective cytokines or nitric acid donors [13–15]. Hence, these molecules might be ideal candidates for re-purposing strategies of well-established and marketed drugs.

Azelastine is a racemate and is being sold and used as such. It is thought to be metabolized to a mixture of mono-hydroxylated 6–hydroxy-azelastine and 7–hydroxy-azelastine, respectively, but also by rat liver microsomes to the corresponding *N*-oxides. However, the literature on the latter is sparse, and published results even more. For example, U. Heinemann et al. in 2003 reported an electrophoretic separation of the stereo- and regioisomeric azelastine metabolites [16]. A resolution of parent compound azelastine was performed on a conalbumin column [17], and the stereoisomers were detected by elaborate frit-FAB LC-MS techniques [18]. Furthermore, the concentration of the drug was measured in human plasma by liquid chromatography coupled to tandem mass spectrometry [19,20]. The isolated stereoisomers, however, were up to now not obtained on a preparative scale, and the *N*-oxides were not even characterized in detail at all.

Since azeleastine already holds one stereogenic center; thus, its oxidation to the corresponding *N*-oxides is expected to result in a total of four stereoisomers. In order to provide at least the respective diastereomers for further evaluation, a robust synthesis method was called for allowing to obtain the respective *N*-oxides in high yields on a preparative scale, and to allow the determination of the configuration of the respective stereoisomers. Regioselective oxidation of the azepane nitrogen can be expected due its high nucleophilicity [21].

2. Results and discussion

N-oxides can be obtained by oxidation from the corresponding amines by a variety of methods but using hydrogen peroxide seemed particularly attractive to us. Hydrogen peroxide is one of the oldest oxidants, it is commercially cheap to acquire, easy to use, and no messy by-products are obtained from its decay. Excess of the oxidant can be destroyed by a variety of methods including heat, pH changes, enzymatically, by adding metal salts or MnO_2.

* Corresponding author.
E-mail address: rene.csuk@chemie.uni-halle.de (R. Csuk).

https://doi.org/10.1016/j.molstruc.2021.132033

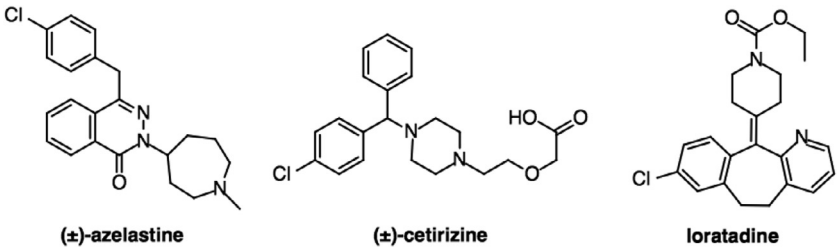

Fig. 1. Structure of most-sold 2nd generation antihistaminic drugs azelastine, cetirizine and loratadine.

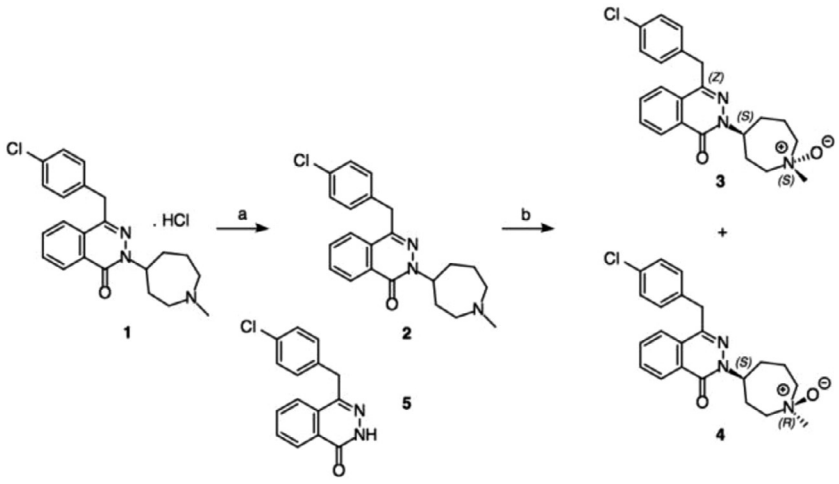

Scheme 1. Synthesis of the *N*-oxides: (*SS*/*RR*)–**3** (*S,S* shown), (*SR*/*RS*)–**4** (*S,R* shown), and MS fragmentation product **5**.

As with all oxidizing agents, proper safety precautions must be observed.

Commercial azelastine hydrochloride (**1**) was therefore converted to the free base **2** (Scheme 1), the reaction of which with hydrogen peroxide led to a mixture of the diastereomeric *N*-oxides (*SS,RR*)–**3** and (*SR,RS*)–**4**, which were easily separated by chromatography. These compounds were characterized in their ESI-MS spectra by *m/z* 398 that corresponds to the presence of a quasi-molecular ion $[M + H]^+$. The isotopic distribution pattern corresponded to the expected values, too. The data from micro-analyses confirmed a molecular formula of $C_{22}H_{24}ClN_3O_2$ as a mono hydrate. Neither IR, MS nor NMR experiments allowed to assign the absolute configuration of these molecules. A superimposition of the respective ^1H and ^{13}C NMR spectra is depicted in Figs. 2 and 3. 2D NMR spectra, however, allowed the assignment of all signals. In the ESI-MS spectra an additional signal was found at *m/z* 271.27 corresponding to the presence of a $[C_{15}H_{11}ClN_2O_2 + H]^+$ fragment, a 8-(4-chlorobenzyl)–4-oxo-3,4-dihydrophthalazin-2-ium ion (unprotonated form **5** depicted in Scheme 1) resulting from the fragmentation of the parent molecular ion (as shown by a MS^2 experiment).

Hence, crystals of **3** were grown, and we succeeded in obtaining crystals suited for an investigation by single crystal X-ray crystallography, the results of which are depicted in Figs. 4 and 5. The supplementary crystallographic data can be obtained free of charge from The Cambridge Crystallographic Data centre via www.ccdc.cam.ac.uk/data_request/cif with CCDC 2,080,715.

Colorless single crystals of the title compound were grown by slow evaporation of a saturated solution in aqueous acetonitrile. Compound **3** forms triclinic crystals, space group $P\bar{1}$, $Z = 2$. The asymmetric unit contains one molecule **3** and one water molecule.

Table 1
Parameters of the hydrogen bonds (pm) in azelastine *N*-oxide • H_2O_3. Symmetry operator i: 1-x, -y, 1-z.

Donor–H....Acceptor	H...A	D...A	∢(D–H...A)
O3–H25..O2	185	268.8(2)	171
O3–H26..O1^i	204	287.8(2)	170

Due to the presence of a crystallographic center of inversion the crystal structure contains both enantiomers of 3 (*R,R* and *S,S*) as a racemate. Bond lengths and angles are within the expected ranges. The seven-membered ring C16-C21-N3 exhibits twist-chair conformation with the nitrogen atom N2 attached to C16 and the carbon atom C22 attached to N3 in equatorial positions. The seven-membered ring attached to N2 and the phenyl ring C1-C6 adopt a nearly parallel orientation roughly perpendicular to the rigid phthalazinone unit. This type of "hair pin" conformation was also observed in azelastine (along with a second conformer) [22] and different solvates of azelastine hydrochloride [23]. The supramolecular structure is characterized by hydrogen bridges between the water molecule as hydrogen donor and the oxygen atoms of the keto (O1) and the nitroxyl groups (O2) as acceptors (Table 1, Fig. 5). As a result, a centrosymmetric ring containing two azelastine *N*-oxide and two water molecules with $R^4_4(22)$ topology is formed.

Since toxicity issues are of high interest for metabolites of established drugs, products **3** and **4** were subjected to cytotoxicity studies (SRB assays). For all human cancer cell lines used (A375, HT29, MCF7, A2780, HeLa) as well as non-malignant cell lines (NIH 3T3, HEK293), EC_{50} values > 30 μM were measured, hence, cytotoxicity issues for these compounds are generally regarded to be not relevant.

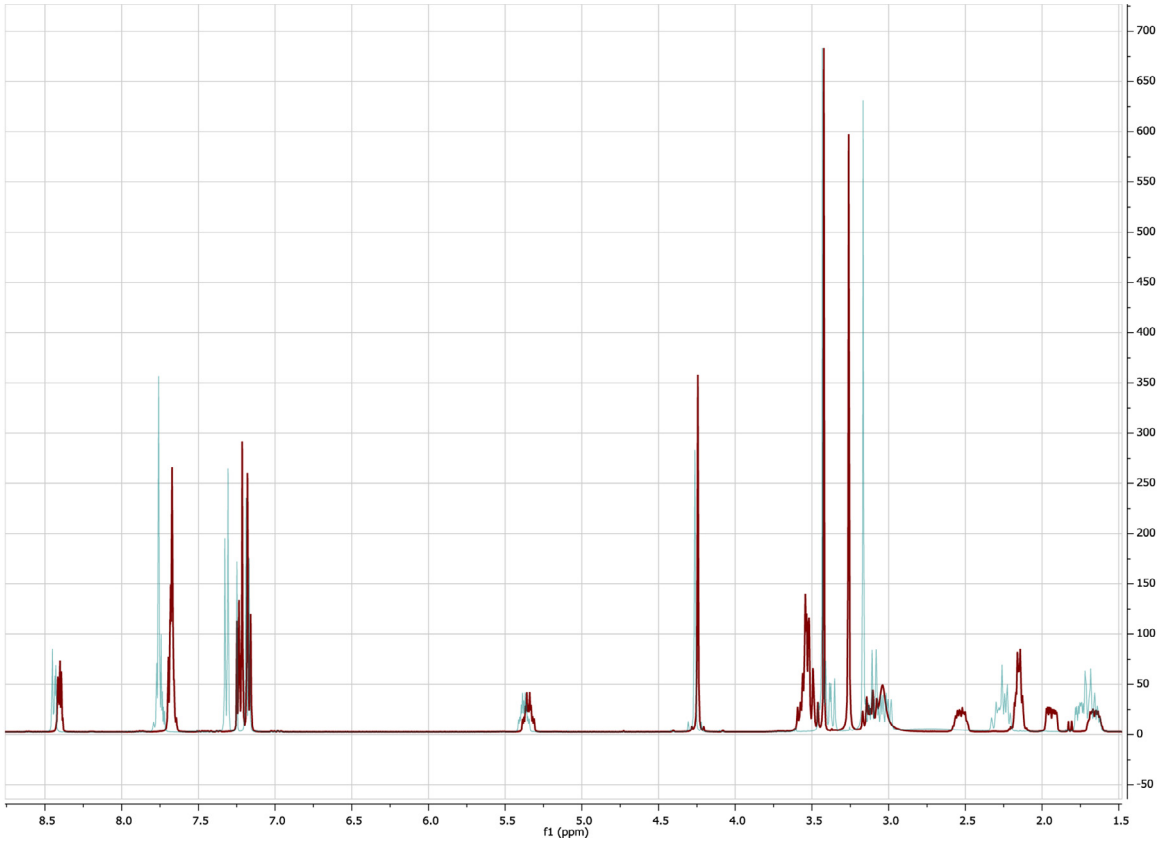

Fig. 2. Superimposed ^{1}H NMR-spectra of (*SS*/*RR*) azelastine *N*-oxide (blue) and (*SR*/*RS*) azelastine *N*-oxide (red) (For interpretation of the references to color in this figure legend, the reader is referred to the web version of this article.).

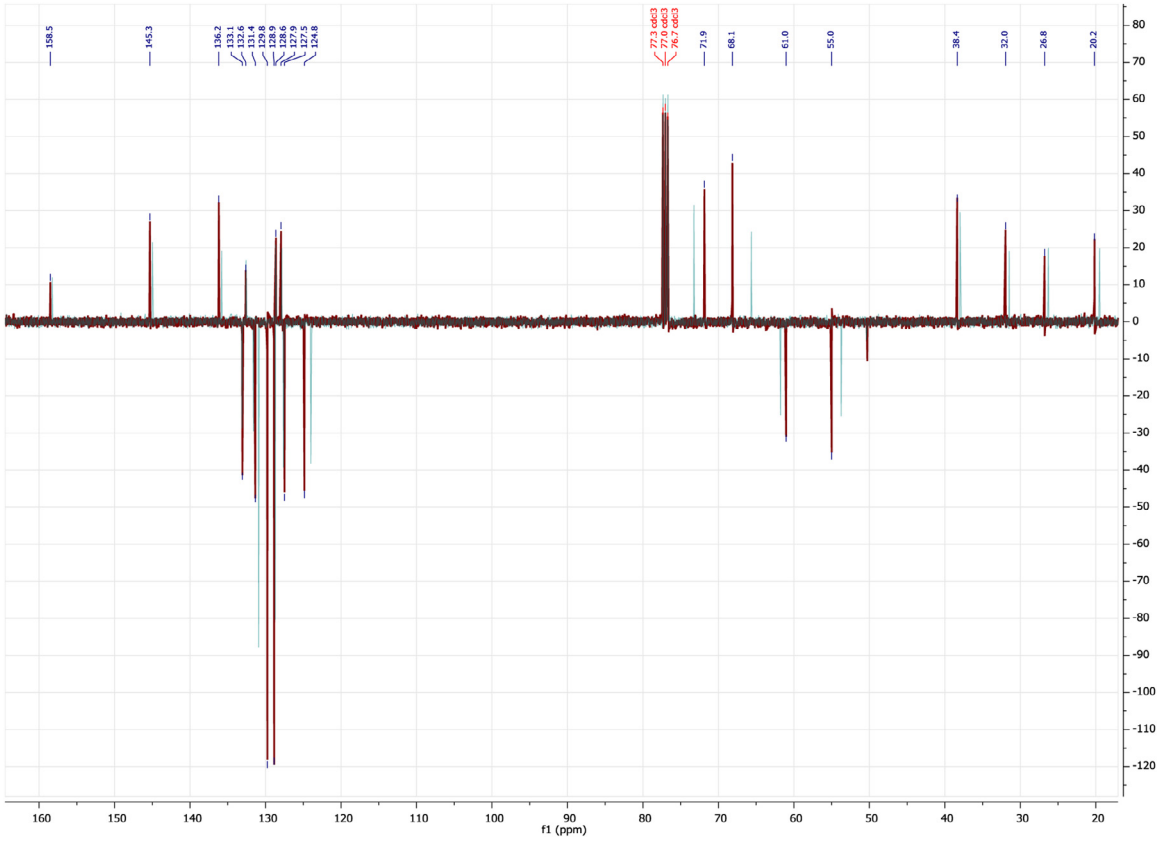

Fig. 3. Superimposed ^{13}C APT NMR spectra of (*SS*/*RR*) azelastine *N*-oxide (**3**, blue) and (*SR*/*RS*) azelastine *N*-oxide (**4**, red) (For interpretation of the references to color in this figure legend, the reader is referred to the web version of this article.).

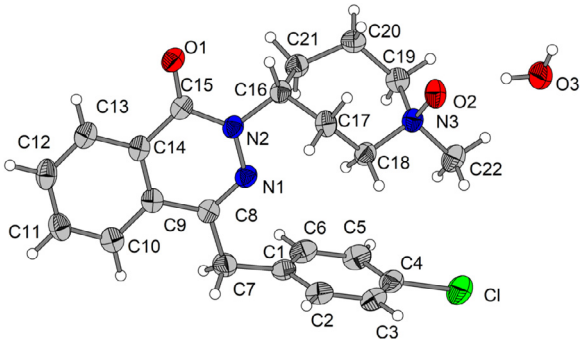

Fig. 4. Molecule structure of the (*R,R*)-enantiomer of azelastine *N*-oxide • H_2O 3 in the crystal showing the labeling scheme. Thermal ellipsoids are at the 50% probability level. Selected bond lengths (pm) and angles (°): C4—Cl 175.6(2), C8—N1 128.4(2), N1—N2 137.1(2), C15—N2 137.4(2), C15—O1 123.2(2), C16—N2 147.9(2), N3—O2 138.4(2), C1—C7—C8 114.8(2) C8—N1—N2 119.2(2).

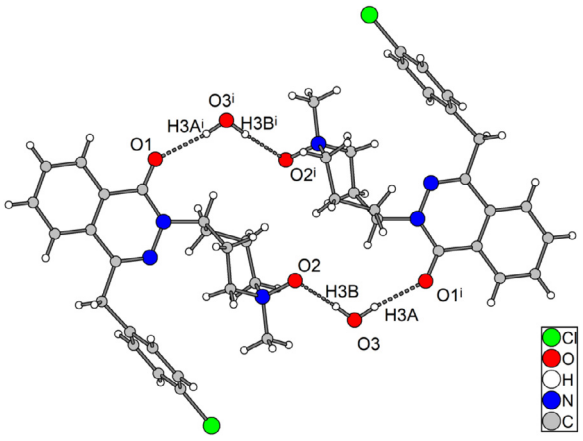

Fig. 5. Section of the crystal structure of azelastine *N*-oxide • H_2O **3** showing the hydrogen bond network. Symmetry operator i: 1-x, -y, 1-z.

Table 2
Crystallographic data for azelastine *N*-oxide • H_2O 3.

Molecular formula	$C_{22}H_{24}ClN_3O_2$ • H_2O
Formula weight /g·mol^{-1}	415.91
Crystal system	triclinic
Space group	P$\bar{1}$
a /pm	854.14(8)
b /pm	989.85(7)
c /pm	1270.3(1)
α /°	100.001(6)
β/°	93.698(7)
γ /°	117.987(6)
Cell volume /nm^3	1.0285(2)
Molecules per cell *Z*	2
Calc. density ρ /g·cm^{-3}	1.343
μ (Mo-*Ka*) /mm^{-1}	0.215
Crystal size /mm	0.41 × 0.39 × 0.11
Diffractometer	STOE IPDS 2
T /K	170
θ range /°	1.65 – 25.0
Absorption correction	none
Reflections collected	8496
Reflections unique	3616
Reflections with $F_o > 4\sigma(F_o)$	2692
Completeness of dataset/%	99.9
R_{int}	0.0458
Parameters	266
R_1 ($I > 2\sigma(I)$)	0.0394
*wR*2 (all data)	0.1070
GooF (*F*2)	1.029

3. Conclusion

A concise synthesis for the large-scale preparation of *rac*. azelastine *N*-oxides **3** and **4** from parent azelastine hydrochloride (**1**) using H_2O_2 is reported. These compounds were easily separated by chromatography, and their structures were confirmed by spectroscopic techniques. An additional X-ray analysis of **3** allowed the assignment of its absolute configuration.

4. Experimental

4.1. General

NMR spectra were recorded using the Agilent spectrometers DD2 500 MHz and VNMRS 400 MHz (δ given in ppm, J in Hz; typical experiments: APT, H–H-COZY, gHMBC, gHSQC, NOESY; calibration to the signal of the deuterated solvent), MS spectra were taken on a Finnigan MAT LCQ 7000 (electrospray, voltage 4.1 kV, sheath gas nitrogen) instrument or on an Advion Expression CMS instrument. TLC was performed on silica gel (Macherey-Nagel, detection with cerium molybdate reagent); melting points are uncorrected (Leica hot stage microscope, or BÜCHI melting point M-565), and elemental analyses were performed on a Foss- Heraeus Vario EL (CHNS) unit. IR spectra were recorded on a Perkin Elmer FT-IR spectrometer Spectrum 1000 or on a Perkin-Elmer Spec- trum Two (UATR Two Unit). The solvents were dried according to usual procedures.

4.2. Crystallographic details

The crystal structure was solved with SHELXT [24] using direct methods and refined with SHELXL [25]. OLEX2 was used as graphical interface [26]. Carbon bound hydrogen atoms and the hydrogen atoms of the water molecule were positioned geometrically at idealized positions and refined using a riding model. The molecular drawings were created with the program DIAMOND [27].

4.3. Synthesis of azelastine N-oxides (3, 4)

To a suspension of azelastine hydrochloride (**1**, 55.0 g, 0.14 mol) in ammonium hydroxide solution (25% in H_2O, 100 mL) was added DCM (100 mL), and the mixture was stirred for 10 min. The organic phase was separated, and the aqueous phase was extracted with DCM (3 × 100 mL). The combined organic phases were evaporated to dryness to yield azelastine base (**2**, 53.77 g, 0.14 mol) as a white amorphous powder. Compound **2** (53.77 g, 0.14 mol) was dissolved in methanol (200 mL) at 50 °C, and an aqueous solution of hydrogen peroxide (35%, 35.4 g, 0.36 mol) was added over a period of 20 min under stirring. The reaction was stirred for another 4 h at 50 °C, and to the resulting clear solution water (150 mL) was added. The methanol was removed under diminished pressure, and the resulting aqueous phase was saturated with sodium chloride. After extraction with DCM (2 × 300 mL), the combined organic phases were washed with water (150 mL), dried over $MgSO_4$, and evaporated to dryness. After column chromatography (1.5 kg, SiO_2, DCM:MeOH:NH_4OH (25% in H_2O), 80:10:1), **3** (26.0 g, 65 mmol), and **4** (16.6 g, 42 mmol), as well as mixture (9.0 g) of both were obtained each as a white powder. *Re*-chromatography of the mixture yielded both diastereomers in almost quantitative yields.

Data for (*SS*/*RR*) azelastine *N*-oxide (**3**, *rac (SS/RR)* 4-(4-(4-chlorobenzyl)−1-oxophthalazin-2(1*H*)-yl)−1-methylazepane 1-oxide): m.p. 154.2 °C; R_F = 0.41 (DCM:MeOH:NH_4OH, 80:10:1); IR (ATR): ν = 3037 *w*, 2955 *w*, 2937 *w*, 2864 *w*, 2768 *w*, 2598 *w*, 1634 *vs*, 1610 *w*, 1588*s*, 1557 *vw*, 1491 *m*, 1464 *m*, 1443 *w*, 1427 *w*, 1407 w, 1387 *w*, 1353 *m*, 1344 *m*, 1334 *m*, 1299 *vw*, 1284 *w*, 1268 *w*, 1233 *vw*, 1183 *w*, 1173 *w*, 1148 *w*, 1104 *w*, 1092 *w*,

1083 *w*, 1048 *m*, 1032 *w*, 1012 *w*, 998 *w*, 976 *vw*, 961 *w*, 939 *w*, 926 *w*, 911 *m*, 875 *m*, 846 *w*, 828 *w*, 814 *m*, 799 *w*, 792 *w*, 782 *vs*, 736 *m*, 721 *w*, 693 *s*, 677 *w*, 639 *w*, 615 *w*, 592 *m*, 581 *w*, 547 *vw*, 515 *w*, 504 *w*, 486 *m* cm^{-1}; UV/Vis (MeOH): λ_{max} (log ε) = 211 (4.42) nm, 290 (3.6) nm, 246 (3.59) nm, 256 (3.55) nm; ^1H NMR (400 MHz, $CDCl_3$): δ = 8.48–8.42 (m, 1H, 13-H), 7.81–7.72 (m, 3H, 10-*H* + 11-*H* + 12-H), 7.35–7.30 (m, 2H, 3-*H* + 5-H), 7.21–7.16 (m, 2H, 2-*H* + 6-H), 5.39 (dddd, *J* = 10.5, 7.0, 7.0, 3.4 Hz, 1H, 16-H), 4.27f (d, *J* = 1.5 Hz, 2H, 7-H_2), 3.48–3.43 (m, 1H, 19-H_a), 3.43–3.35 (m, 1H, 18-H_a), 3.18 (s, 3H, 23-H_3), 3.18–3.13 (m, 1H, 21-H_a), 3.13–3.08 (m, 1H, 19-H_b), 3.08–2.98 (m, 1H, 18-H_b), 2.36–2.20 (m, 2H, 17-H_a + 20-H_b), 1.80–1.62 (m, 3H, 17-H_b + 20-H_b + 21-H_b) ppm; ^{13}C NMR (101 MHz, $CDCl_3$): δ = 158.3 (C-15), 145.0 (C-8), 135.8 (C-1), 133.1 (C-11), 132.6 (C-4), 131.6 (C-10), 130.9 (C-2 + C-6), 128.7 (C-3 + C-5), 128.7 (C-9), 127.8 (C-13), 127.6 (C-14), 124.0 (C-12), 73.2 (C-19), 65.6 (C-18), 61.8 (C-22f), 53.7 (C-16), 38.0 (C-7), 31.5 (C-17), 26.3 (C-21), 19.5 (C-20) ppm; MS (ESI, MeOH): *m/z* = 398.20 ($[M + H]^+$, 100%), 795.20 ($[2M+H]^+$, 30%); analysis calcd for $C_{22}H_{24}ClN_3O_2$. H_2O (415.91): C 63.53, H 6.30, N 10.10; found: C 63.29, H 6.57, N 9.94.

Data for (*SR*/*RS*) azelastine *N*-oxide (**4**, *rac (SR/RS)* 4-(4-(4-chlorobenzyl)−1-oxophthalazin-2(1*H*)-yl)−1-methylazepane 1-oxide)): m.p. 57.7 °C; R_F = 0.30 (DCM:MeOH:NH_4OH, 80:10:1); IR (ATR): ν = 2937 *w*, 2868 *w*, 1641 *vs*, 1610 *w*, 1583*s*, 1551 *vw*, 1489 *m*, 1451 *m*, 1409 *w*, 1386 *w*, 1346 *m*, 1327 *m*, 1267 *vw*, 1217 *vw*, 1180 *w*, 1156 *w*, 1107 *w*, 1089 *m*, 1058 *w*, 1032 *w*, 1015 *m*, 971 *vw*, 934 *w*, 911 *w*, 897 *vw*, 849 *w*, 797 *s*, 775 *m*, 751 *w*, 723 *m*, 690 *s*, 671 *w*, 561 *m*, 482 *m* cm^{-1}; UV/Vis (MeOH): λ_{max} (log ε) = 210 (4.31) nm, 290 (3.55) nm, 256 (3.47) nm; ^1H NMR (400 MHz, $CDCl_3$): δ = 8.42 (ddd, *J* = 7.9, 4.0, 2.4 Hz, 1H, 13-H), 7.72–7.64 (m, 3H, 10-*H* + 11-*H* + 12-H), 7.27–7.20 (m, 2H, 3-*H* + 5-H), 7.20–7.15 (m, 2H, 2-*H* + 6-H), 5.36 (dddd, *J* = 11.3, 7.8, 7.7, 3.7 Hz, 1H, 16-H), 4.25 (s, 2H, 7-H_2), 3.63–3.45 (m, 4H, 18-H_2 + 19-H_2), 3.27 (s, 3H, 22-H_3), 3.20–3.07 (m, 1H, 21-H_a), 2.61–2.47 (m, 1H, 20-H_a), 2.25–2.08 (m, 2H, 17-H_2), 1.95 (ddd, *J* = 15.9, 7.6, 3.7 Hz, 1H, 21-H_b), 1.74–1.60 (m, 1H, 20-H_b) ppm; ^{13}C NMR (101 MHz, $CDCl_3$): δ = 158.5 (C-15), 145.3 (C-8), 136.2 (C-1), 133.1 (C-11), 132.6 (C-4), 131.4 (C-10), 129.8 (C-2 + C-6), 128.9 (C-3 + C-5), 128.6 (C-9), 127.9 (C-14), 127.5 (C-13), 124.9 (C-12), 71.9 (C-19), 68.2 (C-18), 61.0 (C-22), 55.0 (C-16), 38.4 (C-7), 32.0 (C-17), 26.8 (C-21), 20.2 (C-20) ppm; MS (ESI, MeOH): *m/z* = 398.20 ($[M + H]^+$, 100%), 795.20 ($[2M+H]^+$, 25%); analysis calcd for $C_{22}H_{24}ClN_3O_2$. H_2O (415.91): C 63.53, H 6.30, N 10.10; found: C 63.35, H 6.64, N 9.89.

Declaration of Competing Interest

The authors declare that they have no known competing financial interests or personal relationships that could have appeared to influence the work reported in this paper.

CRediT authorship contribution statement

Benjamin Brandes: Visualization. **Jan H. Halz:** Visualization. **Kurt Merzweiler:** Conceptualization, Supervision, Validation, Writing – review & editing. **Hans-Peter Deigner:** Conceptualization, Supervision, Validation, Writing – review & editing. **René Csuk:** Conceptualization, Supervision, Validation, Writing – review & editing.

Acknowledgement

We like to thank Dr D. Ströhl, and Y. Schiller for the NMR spectra, the late Dr. R. Kluge and Th. Schnidt for MS spectra. IR, UV/vis spectra and micro-analysis were recorded by M. Schneider. We are grateful to S. Hoenke for performing the SRB assays (employing cell lines provided by the Department of Oncology) and to Mylan Germany GmbH for a generous donation of azelastine hydrochloride.

Supplementary materials

Supplementary material associated with this article can be found, in the online version, at doi:10.1016/j.molstruc.2021.132033.

References

[1] L. Klimek, A. Sperl, S. Becker, R. Moesges, P.V. Tomazic, Current therapeutical strategies for allergic rhinitis, Expert Opin. Pharmacother. 20 (2019) 83–89.
[2] W. McNeely, L.R. Wiseman, Intranasal azelastine: a review of its efficacy in the management of allergic rhinitis, Drugs 56 (1998) 91–114.
[3] https://www.globenewswire.com/news-release/2019/08/26/1906706/0/en/Akorn-Receives-FDA-Approval-for-Azelastine-Hydrochloride-Nasal-Spray-0-15.html, last accessed 13.10.2021 2021.
[4] https://www.google.com/url?sa=t&rct=j&q=&esrc=s&source=web&cd=&ved=2ahUKEwi35Yb8g5zxAhXwgP0HHW8hC9AQFjABegQIBBAD&url=https%3A%2F%2Fwww.drks.de%2Fdrks_web%2FPdfDownstreamServlet%3FID%3DDRKS00024520%26LOCALE%3Den&usg=AOvVaw2ANPJ7qbYgJqfNh52h9AmT, last accessed 13.10.2021
[5] M.M. Ghahremanpour, J. Tirado-Rives, M. Deshmukh, J.A. Ippolito, C.H. Zhang, I. Cabeza de Vaca, M.E. Liosi, K.S. Anderson, W.L. Jorgensen, Identification of 14 known drugs as inhibitors of the main protease of SARS-CoV-2, ACS Med. Chem. Lett. 11 (2020) 2526–2533.
[6] H.F. Hu, W.W. Xu, Y.J. Li, Y. He, W.X. Zhang, L. Liao, Q.H. Zhang, L. Han, X.F. Yin, X.X. Zhao, Y.L. Pan, B. Li, Q.Y. He, Anti-allergic drug azelastine suppresses colon tumorigenesis by directly targeting ARF1 to inhibit IQGAP1 -ERK-Drp1 -mediated mitochondrial fission, Theranostics 11 (2021) 1828–1844.
[7] R. Jain, S. Mujwar, Repurposing metocurine as main protease inhibitor to develop novel antiviral therapy for COVID-19, Struct. Chem. 31 (2020) 2487–2499.
[8] K. Prerna, V.K. Dubey, Virtual screening and repurposing of FDA-approved drugs from ZINC database to identify potential autophagy inhibitors exploiting autophagy related 4A cysteine peptidase as a target: potential as novel anti-cancer molecule, J. Biomol. Struct. Dyn. (2021) Ahead of Print, doi:10.1080/07391102.2020.1869100.
[9] L.R. Reznikov, M.H. Norris, R. Vashisht, A.P. Bluhm, D. Li, Y.S.J. Liao, A. Brown, A.J. Butte, D.A. Ostrov, Identification of antiviral antihistamines for COVID-19 repurposing, Biochem. Biophys. Res. Commun. 538 (2021) 173–179.
[10] J. Wang, X. Zhang, A.B. Omarini, B. Li, Virtual screening for functional foods against the main protease of SARS-CoV-2, J. Food Biochem. 44 (2020) e13481.
[11] X. Xiao, C. Wang, D. Chang, Y. Wang, X. Dong, T. Jiao, Z. Zhao, L. Ren, C.S. Dela Cruz, L. Sharma, X. Lei, J. Wang, Identification of potent and safe antiviral therapeutic candidates against SARS-CoV-2, bioRxiv (2020) 1–34.
[12] L. Yang, R.J. Pei, H. Li, X.N. Ma, Y. Zhou, F.H. Zhu, P.L. He, W. Tang, Y.C. Zhang, J. Xiong, S.Q. Xiao, X.K. Tong, B. Zhang, J.P. Zuo, Identification of SARS-CoV-2 entry inhibitors among already approved drugs, Acta Pharmacol. Sin. 42 (2020) 1–7.
[13] G.F. Dos Santos Fernandes, A.R. Pavan, J.L. Dos Santos, Heterocyclic N-oxides - a promising class of agents against tuberculosis, Malar. Negl. Trop. Dis. 24 (2018) 1325–1340.
[14] L.L. Fershtat, E.S. Zhilin, Recent advances in the synthesis and biomedical applications of heterocyclic NO-donors. LID - doi:10.3390/molecules26185705.
[15] A.M. Mfuh, O.V. Larionov, Heterocyclic N-oxides - an emerging class of therapeutic agents, Curr. Med. Chem. 22 (2015) 2819–2857.
[16] U. Heinemann, G. Blaschke, N. Knebel, Simultaneous enantioselective separation of azelastine and three of its metabolites for the investigation of the enantiomeric metabolism in rats I. Liquid chromatography-ionspray tandem mass spectrometry and electrokinetic capillary chromatography, J. Chromatogr. B Anal. Technol. Biomed. Life Sci. 793 (2003) 389–404.
[17] N. Mano, Y. Oda, T. Miwa, N. Asakawa, Y. Yoshida, T. Sato, Conalbumin-conjugated silica gel, a new chiral stationary phase for high-performance liquid chromatography, J. Chromatogr. 603 (1992) 105–109.
[18] N. Mano, H. Oda, N. Asakawa, Y. Yoshida, T. Sato, Resolution of 4-(4-chlorobenzyl)-2-(hexahydro-1-methyl-1H-azepin-4yl)-1(2H)-phthalazinone enantiomers in plasma with frit-FAB LC-MS using a conalbumin column, J. Pharm. Biomed. Anal. 12 (1994) 557–567.
[19] Y.S. Park, S.H. Kim, Y.J. Kim, S.C. Yang, M.H. Lee, C.M. Shaw, J.S. Kang, Determination of Azelastine in human plasma by validated liquid chromatography coupled to tandom mass spectrometry (LC-ESI/MS/MS) for the clinical studies, Int. J. Biomed. Sci. 6 (2010) 120–127.
[20] W. Zha, L. Shum, Simultaneous determination of azelastine and its major metabolite desmethylazelastine in human plasma using high performance liquid chromatography-tandem mass spectrometry, J. Chromatogr. B Anal. Technol. Biomed. Sci. 906 (2012) 69–74.
[21] R.M.B. Dyer, P.L. Hahn, M.K. Hillinsky, Selective heteroaryl N-oxidation of amine-containig molecules, Org. Lett. 20 (2018) 2011–2014.
[22] G. Scheffler, J. Engel, B. Kutscher, W.S. Sheldrick, P. Bell, Synthesis and X-Ray-structure analysis of Azelastine, Arch Pharm. 321 (1988) 205–208.
[23] E. Maccaroni, E. Alberti, L. Malpezzi, G. Razzetti, C. Vladiskovic, N. Masciocchi, Azelastine hydrochloride: a powder diffraction and C-13 CPMAS NMR study of its anhydrous and solvated forms, Cryst. Growth Des. 9 (2009) 517–524.

[24] G.M. Sheldrick, SHELXT-integrated space-group and crystal structure determination, Acta Crystallogr. A 71 (2015) 3–8 2015.
[25] G.M. Sheldrick, Crystal structure refinement with SHELXL, Acta Crystallogr. C 71 (2015) 3–8.
[26] O.V. Dolomanov, L.J. Bourhis, R.J. Gildea, J.A.K. Howard, H. Puschmann, OLEX2: a complete structure solution, refinement and analysis program, J. Appl. Crystallogr. 42 (2009) 339–341.
[27] K. Brandenburg, K.: DIAMOND. Visual Crystal Structure Information System, Crystal Impact, Bonn, Germany, 2021 Ver. 4.6.5.